N71-25439

NASA TECHNICAL MEMORANDUM

NASA TM X-2263

NASA TM X-2263

CASE FILE COPY

SOME LIMITATIONS ON ION-CYCLOTRON WAVE GENERATION AND SUBSEQUENT ION HEATING IN MAGNETIC BEACHES

by Donald R. Sigman

Lewis Research Center

Cleveland, Ohio 44135

NATIONAL AERONAUTICS AND SPACE ADMINISTRATION • WASHINGTON, D. C. • MAY 1971

1. Report No. NASA TM X-2263	2. Government Accession No.	3. Recipient's Catalog No.
4. Title and Subtitle SOME LIMITATIONS ON ION-CYCLOTRON WAVE GENERATION AND SUBSEQUENT ION HEATING IN MAGNETIC BEACHES		5. Report Date May 1971
		6. Performing Organization Code
7. Author(s) Donald R. Sigman		8. Performing Organization Report No. E-6080
		10. Work Unit No. 129-02
9. Performing Organization Name and Address Lewis Research Center National Aeronautics and Space Administration Cleveland, Ohio 44135		11. Contract or Grant No.
		13. Type of Report and Period Covered Technical Memorandum
12. Sponsoring Agency Name and Address National Aeronautics and Space Administration Washington, D. C. 20546		14. Sponsoring Agency Code
15. Supplementary Notes		

16. Abstract

Thermal effects have been included in the analysis of ion-cyclotron waves generated by a Stix coil. Peak power coupling efficiency is reduced whenever ion or electron temperatures are sufficient for ion-cyclotron or Landau damping to occur. Because of the absorption of wave power under the coil, the wave power reaching an external "magnetic beach" is reduced. Other topics discussed include the effect of a Faraday shield on power coupling and wave damping and the interference effects which arise when waves are reflected from the ends of the plasma column.

17. Key Words (Suggested by Author(s)) Ion heating; Ion-cyclotron waves; Magnetic beach; Faraday shield; Cyclotron damping; Landau damping	18. Distribution Statement Unclassified - unlimited

19. Security Classif. (of this report)	20. Security Classif. (of this page)	21. No. of Pages	22. Price*
Unclassified	Unclassified	20	$3.00

*For sale by the National Technical Information Service, Springfield, Virginia 22151

SOME LIMITATIONS ON ION-CYCLOTRON WAVE GENERATION AND SUBSEQUENT ION HEATING IN MAGNETIC BEACHES

by Donald R. Sigman

Lewis Research Center

SUMMARY

Thermal effects have been included in the analysis of ion-cyclotron waves generated by a Stix coil. Peak power coupling efficiency is reduced whenever ion or electron temperatures are sufficient for ion-cyclotron or Landau damping to occur. Because of the absorption of wave power under the coil, the wave power reaching an external "magnetic beach" is reduced. Other topics discussed include the effect of a Faraday shield on power coupling and wave damping and interference effects which arise when waves are reflected from the ends of the plasma column.

INTRODUCTION

In the ideal case, heating of plasma ions by ion-cyclotron waves can be viewed as a three-step process. First, a Stix coil (ref. 1, ch. 5) is used to couple radiofrequency energy to ion-cyclotron waves in a region of the plasma where the frequency of the waves ω is less than the ion-cyclotron frequency Ω_i. Next, the waves propagate away from the Stix coil toward a region of lower magnetic field (called a magnetic beach), where the ion-cyclotron and wave frequencies are nearly equal. Finally, in the magnetic beach region, there are many ions which see the wave field at the cyclotron frequency and thus absorb energy from the wave.

If the plasma ion and/or electron temperature is low underneath the Stix coil and in the immediate vicinity, collisionless damping processes (primarily electron Landau damping and ion-cyclotron damping) are not important; and the efficiency of coupling energy to the waves is very high (refs. 2 and 3). However, if the plasma temperature is raised, there should be a point where electron Landau and/or ion-cyclotron damping will occur underneath the Stix coil. When this happens, it is certainly true that some of the ions will be heated outside of the magnetic beach region and not become trapped in a local mirror surrounding the beach (see fig. 1). It has also been shown (ref. 4) that,

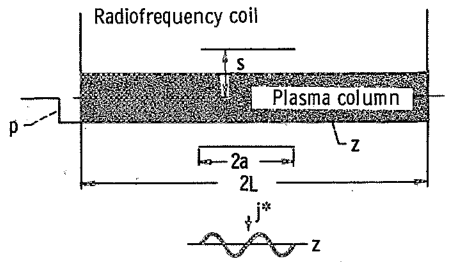

(a) Plasma - radiofrequency-coil geometry and finite-length system.

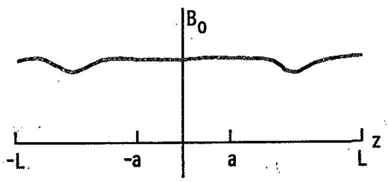

(b) Confining field with beaches.

Figure 1. - Plasma model and direct-current confining magnetic field.

whenever there is damping underneath the coil, the coupling efficiency is changed. At Lewis this change in coupling efficiency has been seen experimentally in the Ion Cyclotron Resonance Apparatus (ICRA II). It was found that increasing the current in the Stix coil (and supposedly raising the temperature of the plasma) did not cause the power coupled to the plasma waves to increase at a rate proportional to the square of the current. Also, an energy balance study of the beach region of ICRA II gives experimental evidence that a significant amount of energy being coupled to the plasma does not reach the ions in the beach.

This report examines the effects of finite plasma temperatures on coupling efficiency and determines the fraction of input energy reaching beach regions. Also, the effect of a Faraday shield on the wave damping is studied. Finally, a method is proposed whereby all the energy leaving the Stix coil can be made to flow in the same direction along the plasma column.

SYMBOLS

a	one-half Stix coil length
$\underline{B}$	wave magnetic field
B_0	direct-current-confining magnetic field

$\underline{E}$	wave electric field
I	Stix coil current
I_0, I_1	modified Bessel functions of the first kind
J_0, J_1	Bessel functions of the first kind
j^*	Stix coil current density
K_0, K_1	modified Bessel functions of the second kind
k	plasma wave number
L	one-half system length
n_e	electron density (equal to deuterium ion density)
P_{in}	power coupled to plasma by Stix coil
P_{out}	power flow from region of Stix coil
p	plasma column radius
R	energy loss rate from magnetic beaches
r	radial position coordinate
s	Stix coil radius
T_e	electron temperature
T_i	deuterium ion temperature
V	volume of magnetic beaches
$v_{\parallel_{i,e}}$	thermal velocity parallel to confining field
$Z(\xi)$	plasma dispersion function
z	axial position coordinate
z_c	axial center position of Stix coil
α_0^e	$\omega/kv_{\parallel_e}$
α_{-1}^i	$(\omega - \Omega_i)/kv_{\parallel}$
θ	aximuthal position coordinate
κ	Boltzmann's constant
λ_0	Stix coil wavelength
ν	radial wave number

ξ	argument of plasma dispersion function
τ	energy loss time for beach regions
Ω	ω/Ω_i
Ω_i	ion-cyclotron frequency
ω	wave frequency

METHOD OF ANALYSIS

The plasma is assumed to be collisionless (ref. 2) and to consist only of deuterium ions and electrons. The particle density and the confining magnetic field are both assumed to be uniform. The ions and electrons are assumed to have Maxwellian velocity distributions, but the temperature of each species may be different. The plasma column is of finite length 2L. The waves are excited by a two-length Stix coil centered at $z = z_c$, where $-L + (\lambda_0/2) < z_c < L - (\lambda_0/2)$ and λ_0 is the wavelength of the Stix coil. When a magnetic beach exists, a negligible amount of the wave energy leaving the Stix coil is reflected back toward the coil and the plasma column appears infinitely long. This condition in the model is simulated by making L much greater than the characteristic damping length of the ion-cyclotron wave (L = 10 m is usually sufficient). Unless otherwise stated, L = 10 meters and $z_c = 0$. However, the effects of placing a reflecting grid near one or both ends of the Stix coil is also discussed briefly.

The wave fields in this finite-length plasma column are represented as a Fourier series in a technique described in more detail in appendix A. There, the wave field equations are presented for two cases: a Faraday shield located at the plasma boundary, and no Faraday shield.

RESULTS AND DISCUSSION

Effect of Finite Ion and Electron Temperature on Coupling Efficiency

Figures 2 and 3 give examples of the effect of finite ion and electron temperatures on wave coupling efficiency. The values of many of the parameters (which are listed on the figures) are typical of those in ICRA II. In figure 2 (where the electron temperature is held fixed at 10 eV), it is seen that coupling efficiency is reduced more than a factor of 3 by increasing the temperature from that of a cold plasma ($T_i = 10$ eV) to that of a hot (but experimentally realizable) plasma ($T_i = 1000$ eV).

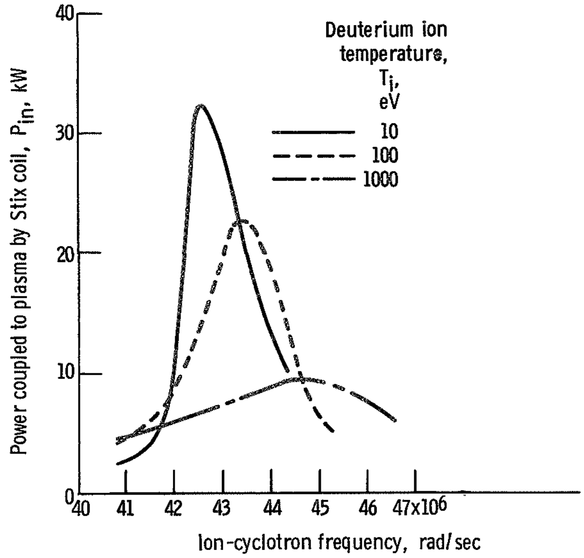

Figure 2. - Power transfer to plasma as function of ion-cyclotron frequency with ion temperature as a parameter. Electron density, 2×10^{12} cm^{-3}; electron temperature, 10 eV; wave frequency, 40.8×10^{6} radians per second; coil current, 100 amperes; coil radius, 7.5 centimeters.

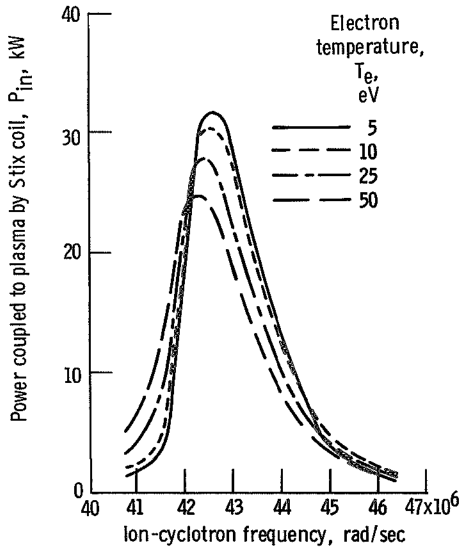

Figure 3. - Power transfer to plasma as function of ion-cyclotron frequency with electron temperature as a parameter. Electron density, 2×10^{12} cm^{-3}; deuterium ion temperature, 0.01 eV; wave frequency, 40.8×10^{6} radians per second; coil current, 100 amperes; coil wavelength, 41 centimeters; coil radius, 7.5 centimeters; plasma radius, 4 centimeters; deuterium gas.

It is expected that ion thermal effects become important when $\alpha^i_{-1} = (\omega - \Omega_i)/kv_{\|_i}$ is of order one or less. Electron thermal effects are important when $\alpha^e_0 = \omega/kv_{\|_e}$ is of order one or less. The respective values of α^i_{-1} (at peak coupling for T_i equal to 10, 100, and 1000 eV are 3.7, 1.8, and 0.8. For the electrons, respective values of α^e_0 for T_e equal to 10 and 50 eV are 1.41 and 0.64.

Figure 4 shows peak coupling efficiency as a function of density (again with T_i as a parameter). At low densities the reduction in coupling due to increased ion temperature

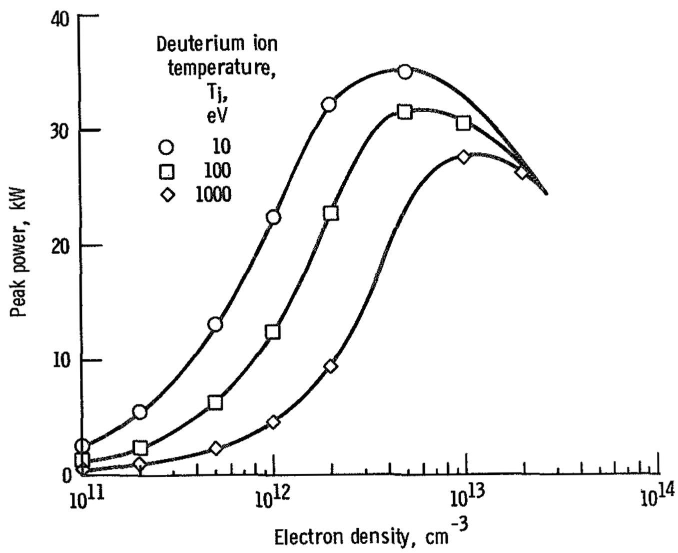

Figure 4. - Peak power transfer to plasma as function of electron density with ion temperature as a parameter. Electron temperature, 10 eV; wave frequency, 40.8×10^6 radians per second; coil current, 100 amperes; coil wavelength, 41 centimeters; coil radius, 7.5 centimeters; plasma radius, 4 centimeters; deuterium gas.

is large. This is because peak coupling occurs for small values of $|\omega - \Omega_i|$. At higher densities, the peak coupling occurs at magnetic fields for which $|\omega - \Omega_i|$ is larger and temperature effects are then less important.

In general, whenever the wave damping length is of the order of, or less than, the Stix coil length, a significant reduction in coupling efficiency occurs.

Energy Absorption Underneath Stix Coil

As was pointed out in the previous section, coupling efficiency is reduced when con-

TABLE I. - RESULTS OF CALCULATIONS OF ENERGY LEAVING AND ABSORBED UNDER A STIX COIL

[Stix coil: radius, s = 7.5 cm; wavelength, λ_0 = 41 cm; rms current, I = 100 A. Plasma radius, p = 4 cm.]

Table row	Axial center position of Stix coil, z_c, cm	Electron density, n_e, cm^{-3}	Deuterium ion temperature, T_i, eV	Electron temperature, T_e, eV	Wave frequency, ω, sec^{-1}	Ratio of wave frequency to ion cyclotron frequency, $\Omega = \omega/\Omega_i$	Faraday shield present?	Power coupled to plasma by Stix coil, P_{in}, kW	Power flow from region of Stix coil, P_{out}, kW	P_{in}/P_{out} ×100, percent
1	0	2×10^{12}	100	10	4.08×10^{7}	[a]0.953	Yes	24.0	4.2	17.5
2					4.08	[b].936	Yes	42.4	17.6	41.5
3					4.08	[b].936	No	29.5	9.4	31.9
4					6.28	[a].953		48.0	18.0	37.5
5					4.08	[a]1.000		3.55	.44	12.3
6		1×10^{13}			4.08	[a].887		10.2	3.6	35.3
7		1×10^{14}	10^4	10^4	1.00×10^{8}	[b].312		60.4	16.6	27.5
8	-950	2×10^{12}	100	10	4.08×10^{7}	[b].933	Yes	68.0	28.4	41.8
9	-950	2	100	10	4.08	[b].933	No	40.3	12.4	30.8

[a]Ω values are greater than those at peak coupling.
[b]Ω values are those at peak coupling.

ditions under the Stix coil are right for either electron Landau damping ($\omega/kv_{\|_e} \sim 1$) or ion-cyclotron damping ($(\omega - \Omega_i)/kv_{\|_i} \sim 1$). Obviously, whenever there is damping under the coil, not all the energy coupled-in leaves the coil region or gets to a magnetic beach located some distance from the coil. The amount of wave energy flowing away from the coil region has been calculated by evaluating the Poynting vector (axial component) at the ends of the Stix coil and integrating over the cross-sectional area of the plasma. The energy absorbed under the Stix coil is then the difference between the energy coupled-in P_{in} and this integral of the Poynting vector P_{out}. The results of these calculations for some typical cases are shown in table I.

Rows 1 and 2 of the table show that operating the Stix coil only slightly further from $\Omega = 1$ (0.936 as opposed to 0.952) can significantly increase the fraction of the input energy which leaves the coil (41.5 percent as opposed to 17.5 percent).

When a Faraday shield is placed at the plasma surface, the wave E_z field is forced to zero there; and subsequently the average E_z field across the whole plasma column is lower. When E_z is less, the wave energy transferred to the electrons through Landau damping is less. This means that not only is the coupling efficiency increased, but also a higher percentage of the energy coupled-in leaves the region of the Stix coil in the form of waves. (Compare rows 2 and 3 and rows 8 and 9.)

Figure 5 shows the Poynting vector and wave E_z and E_r fields for the conditions of rows 2 and 3. Without the Faraday shield the energy flow $\left[\sim (\underline{E} \times \underline{B})_z\right]$ is peaked near the radial boundary, with the peak moving slightly inward as z increases. Placing the Faraday shield at the plasma radius forces both E_r and E_z to be smaller near the surface and causes the energy flow to peak more towards the center of the plasma column.

Row 5 shows that at $\Omega = 1$ both the coupling efficiency ($P_{in} = 3.55$ kW) and the fraction of the input energy leaving the coil (12.3 percent) are low. The frequency of the radiofrequency generator in ICRA II is presently 6.5 megahertz ($\omega = 4.08\times10^{7}\ \mathrm{sec}^{-1}$). A comparison of rows 1 and 4 shows the improvement in performance that might be attained by increasing the frequency roughly 50 percent to 10 megahertz ($\omega = 6.28\times10^{7}\ \mathrm{sec}^{-1}$).

Row 7 gives results of a calculation at conditions similar to those for a fusion reactor. Increasing the density and increasing the temperature both have the effect of reducing the coupling; but this is offset by the necessity of operating further from $\Omega = 1$ (because of high density) and by the use of a larger value of ω (because of the larger confining field of the fusion plasma).

All the calculations presented in figures 1 to 4 and in rows 1 to 7 of table I were made with the Stix coil at the center of a plasma column of length $2L = 20$ meters. With $L = 10$ meters the waves for the conditions studied are damped out significantly by the time they propagate out to $z = L$; and thus there are no reflected waves returning to the Stix coil. When either or both of the ends of the system (which are assumed to be per-

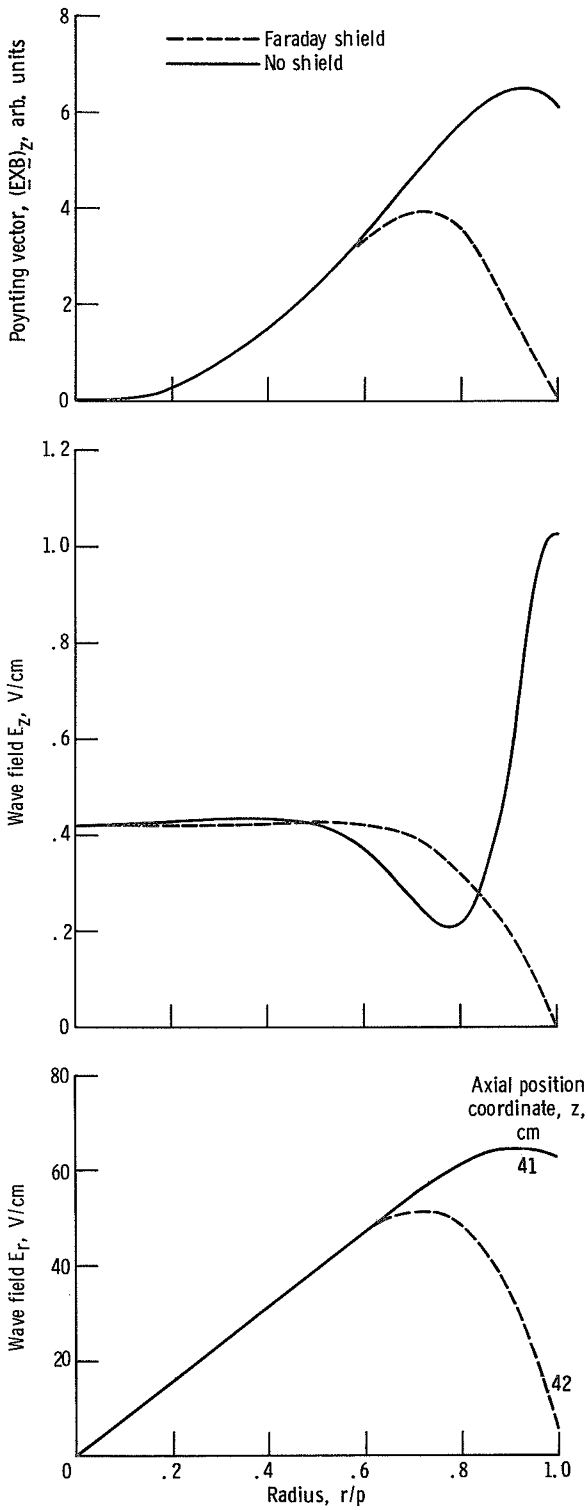

Figure 5. - Poynting vector and wave E_z and E_r fields as function of radius. Electron density, 2×10^{12} cm^{-3}; deuterium ion temperatures, 100 eV; electron temperature, 10 eV; ratio of wave frequency to ion-cyclotron frequency, 0.936; axial position coordinate, 42 centimeters (unless otherwise noted).

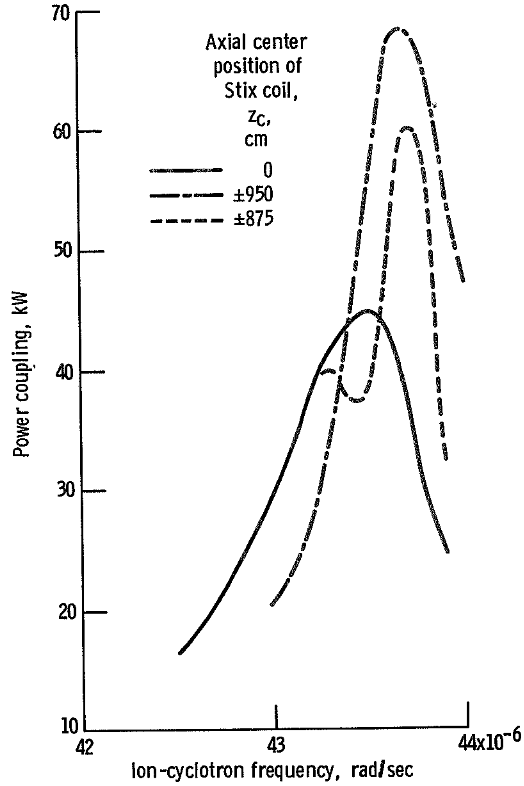

Figure 6. - Power coupling as function of ion-cyclotron frequency with Stix coil center position as a parameter. Electron density, 2×10^{12} cm^{-3}; deuterium ion temperature, 100 eV; electron temperature, 10 eV; coil current, 100 amperes; coil radius, 7.5 centimeters; plasma radius, 4 centimeters; wave frequency, 40.8×10^{6} radians per second; Stix coil wavelength, 41 centimeters; one-half system length, 1000 centimeters; Faraday shield at r = p.

fectly reflecting) are brought close to the ends of the Stix coil, some of the wave energy is reflected back underneath the coil; and interference effects play a role in the coupling process. The result is that the coupling efficiency can be either increased or decreased depending on the position of the ends of the system relative to that of the coil. Figure 6 gives power coupling as a function of Ω_i, with L held at 10 meters and z_c (the position of the center of the Stix coil) as a variable parameter. At $\Omega_i = 4.37\times10^7$ sec^{-1} the coupling is always higher than for the case of $z_c = 0$. The percentage of the energy leaving the Stix coil does not change much (compare rows 8 and 2 or rows 9 and 3 of table I), but it is now all directed out one end of the coil. Thus it seems possible that such a reflector

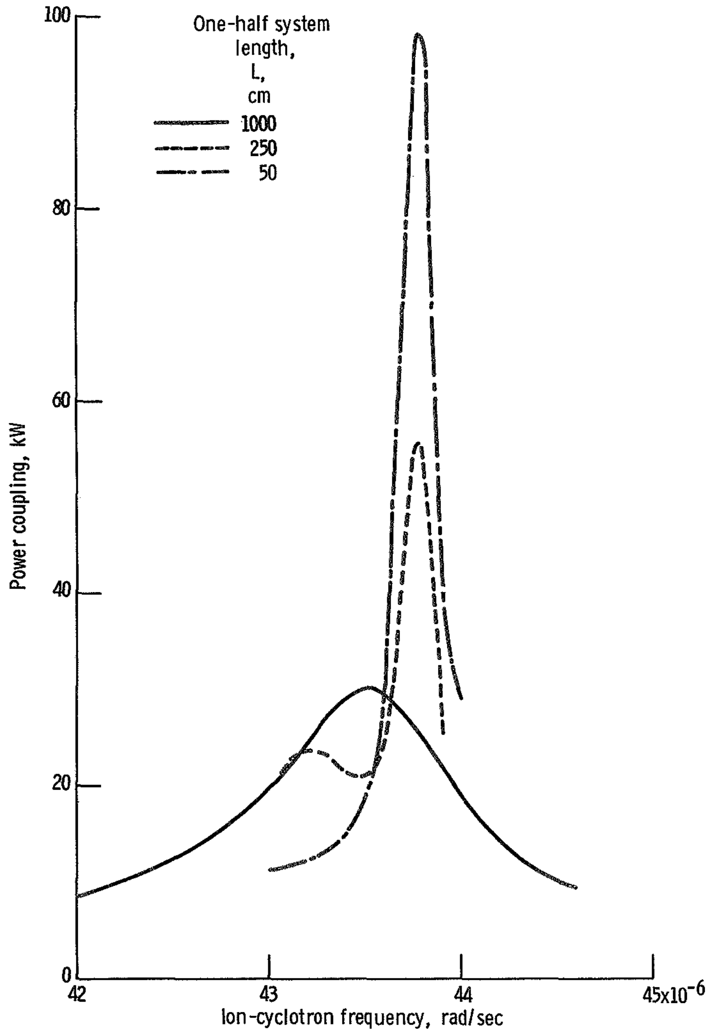

Figure 7. - Power coupling as function of ion-cyclotron frequency with system length as a parameter. Electron density, 2×10^{12} cm^{-3}; deuterium ion temperature, 100 eV; electron temperature, 10 eV; coil current, 100 amperes; plasma radius, 4 centimeters; wave frequency, 40.8×10^6 radians per second; Stix coil wavelength, 41 centimeters; axial center position of Stix coil, 0; no Faraday shield.

at one end of the coil might cause more than twice as much energy to leave the other end of the coil, to be absorbed in a magnetic beach.

Figure 7 gives power coupling as a function of Ω_i with $z_c = 0$ and L as a variable parameter. It is seen that as L becomes less, the interference effects become more pronounced, and there are values of Ω_i where the coupling is much higher than in the case where L = 10 meters. It does not appear that this increased coupling could be taken advantage of in conjunction with a magnetic beach; but it does appear that it could be used for direct heating in the vicinity of the Stix coil.

Energy Balance of Magnetic Beaches

In the magnetic beach regions of ICRA II average ion temperatures of about 300 eV have been achieved with an electron density of 2×10^{12} cm^{-3}. The volume of both beaches is approximately 6000 cm^3. The measured energy loss time τ is about 10^{-4} second. The energy loss rate, then, is approximately

$$R = \frac{n_e(\kappa T_i)V}{\tau} \approx 6 \text{ kilowatts}$$

This compares to an experimental energy input rate at the Stix coil of 26 kilowatts. Row 2 of table I is the best-known approximation to this experiment and predicts that 41.5 percent of the input energy leaves the Stix coil. (41.5 percent of 26 kW is about 11 kW.) These two values (6 and 11 kW) are consistent with each other when it is considered that (1) not all the energy leaving the coil gets to the beaches (which start about 20 cm from the end of the Stix coil) and (2) the parallel ion temperature used for the theoretical calculation is not known to within better than a factor of 2.

CONCLUSIONS

A study has been made of the effect of finite ion and electron temperature on ion-cyclotron waves generated by a Stix coil. Whenever there is strong electron-Landau damping or ion-cyclotron damping underneath the coil, coupling efficiencies are reduced. In a typical plasma ($n_e = 2\times10^{12}$ cm^{-3}, T_i = 100 eV, T_e = 10 eV, and $\omega = 4.08\times10^7$ sec^{-1}) only about 40 percent of the power coupled to the plasma column leaves the region of the Stix coil in the form of ion-cyclotron waves. Thus, the attainable ion temperatures in small local mirrors surrounding magnetic beaches is limited. For plasma conditions close to those of a fusion plasma, coupling efficiencies can still be appreciable; although little power leaves the coil region.

Reflections of waves from the ends of the system cause resonant cavity effects which produce greatly increased coupling efficiencies for certain values of Ω_i. If the Stix coil is near one end of the system, it may be possible to use reflections from that end to aid in increasing coupling efficiency and to direct a higher percentage of the wave power toward a beach region near the other end.

Lewis Research Center,
National Aeronautics and Space Administration,
Cleveland, Ohio, January 14, 1971,
129-02.

APPENDIX A

FOURIER SERIES REPRESENTATION OF STIX COIL FIELDS IN A FINITE-LENGTH PLASMA COLUMN

Assume a uniform plasma column (length 2L, radius p) immersed in a uniform axial magnetic field B_0 and surrounded by a two-wavelength Stix coil (length = $2\lambda_0$, radius = s) centered at z = 0 (see fig. 1). Also, assume the plasma column is bounded on the ends by perfectly conducting plates so that the electric fields (E_r, E_θ) tangential to the plates may be set equal to zero. Consider the E_θ component of the wave field generated by the coil (all other field components can be generated from Maxwell's equations once E_θ is known). The current distribution in the coil j* is asymmetric and can thus be represented by a Fourier sine series. The field E_θ is likewise asymmetric and can also be written as a sine series. Because of superposition, each term in the E_θ series can be thought of as the field related to the corresponding term in the current distribution series. The proper sine series to satisfy $E_\theta = 0$ at $z = \pm L$ is

$$E_\theta(r, z, t) = \sum_{n=0}^{\infty} E_{\theta_n}(r) \sin\left(\frac{n\pi z}{L}\right) e^{i\omega t}$$

and

$$j^*(r, z, t) = \sum_{n=0}^{\infty} j^*_n \delta(r - s) \sin\left(\frac{n\pi z}{L}\right) e^{i\omega t}$$

Notice that, in order to satisfy the boundary condition at $z = \pm L$ for all values of r, it is necessary to make each term in the series equal zero. This is because the radial dependence of each of the coefficients $E_{\theta_n}(r)$ is different.

The Fourier coefficients $E_{\theta_n}(r)$ have been derived previously as a function of j^*_n (ref. 2).

$$E_{\theta_n}(r) = \left[a_1 J_1(\nu_1 r) + a_2 J_1(\nu_2 r)\right] j_n^* \qquad (r < p)$$

$$= \left[b_1 I_1(k_n r) + b_2 K_1(k_n r)\right] j_n^* \qquad (p < r < s)$$

$$= c_2 K_1(k_n r) j_n^* \qquad (r > s)$$

where

$$k_n = \frac{n\pi}{L}$$

$$\nu_{1,2} = \frac{-B \pm \sqrt{B^2 - 4C}}{2}$$

$$B = \frac{k_n^2(P + S)}{2} - \frac{\omega^2}{c^2} P + \frac{\omega^2}{c^2} \frac{(D^2 - S^2)}{S}$$

$$C = \frac{P}{S} k_n^4 - 2 \frac{\omega^2}{c^2} k_n^2 S + \frac{\omega^4}{c^4} (S^2 - D^2)$$

and where S, $-iD$, and P are the hot-plasma dielectric tensor elements K_{xx}, K_{xy} and K_{zz} (ref. 1, ch. 9) (all functions of k_n). The computation of the dielectric tensor required evaluation of the plasma dispersion function $Z(\xi)$. The approximations for $Z(\xi)$ used in this report are found in appendix B. The coefficients a_1, a_2, b_1, b_2, and c_2 can be calculated by first computing the remaining $\underline{E}$ and $\underline{B}$ field components from Maxwell's equations and applying the following boundary conditions:

(1) Tangential components of both $\underline{E}$ and $\underline{B}$ are continuous across the plasma-vacuum interface $(r = p)$.

(2) Tangential components of $\underline{E}$ and $\underline{B}$ are continuous at the external current sheet $(r = s)$, except B_z which is discontinuous by $(4\pi/c)j_n^*$.

(3) When a Faraday shield is assumed to exist at the plasma boundary $(r = p)$, E_z is set equal to zero there and everywhere outside the plasma column.

With no Faraday shield at $r = p$,

$$a_1 = \frac{4\pi i\omega s}{c^2} K_1(ks) \frac{\nu_2 pJ_0(\nu_2 p)\left[I_1(kp) + \delta K_1(kp)\right] - kpJ_1(\nu_2 p)\left[I_0(kp) - \delta K_0(kp)\right]}{\nu_2 pJ_1(\nu_1 p)J_0(\nu_2 p) - \nu_1 pJ_0(\nu_1 p)J_1(\nu_2 p)}$$

$$a_2 = \frac{-4\pi i\omega s}{c^2} K_1(ks) \frac{\nu_1 pJ_0(\nu_1 p)\left[I_1(kp) + \delta K_1(kp)\right] - kpJ_1(\nu_1 p)\left[I_0(kp) - \delta K_0(kp)\right]}{\nu_2 pJ_1(\nu_1 p)J_0(\nu_2 p) - \nu_1 pJ_0(\nu_1 p)J_1(\nu_2 p)}$$

$$\delta = \frac{\alpha_1\left[\gamma\nu_1 pJ_0(\nu_1 p) + PJ_1(\nu_1 p)\right]J_1(\nu_2 p) - \alpha_2\left[\gamma\nu_2 pJ_0(\nu_2 p) + PJ_1(\nu_2 p)\right]J_1(\nu_1 p)}{kpK_0(kp)K_1(kp)\Gamma_a}$$

$$\Gamma_a = \alpha_1\left[\gamma\nu_1 pJ_0(\nu_1 p) + PJ_1(\nu_1 p)\right]\left[\gamma\nu_2 pJ_0(\nu_2 p) + J_1(\nu_2 p)\right]$$

$$- \alpha_2\left[\gamma\nu_2 pJ_0(\nu_2 p) + PJ_1(\nu_2 p)\right]\left[\gamma\nu_1 pJ_0(\nu_1 p) + J_1(\nu_1 p)\right]$$

$$\gamma = \frac{K_1(kp)}{kpK_0(kp)}$$

$$\alpha_1 = \frac{S\left(k^2 + \nu_1^2\right) - \dfrac{\omega^2}{c^2}(S^2 - D^2)}{kD}$$

$$\alpha_2 = \frac{S\left(k^2 + \nu_2^2\right) - \dfrac{\omega^2}{c^2}(S^2 - D^2)}{kD}$$

With a Faraday shield at $r = p$,

$$a_1 = \frac{4\pi i\omega s}{c^2}\frac{K_1(ks)\alpha_2\nu_2 pJ_0(\nu_2 p)}{\Gamma_b}$$

$$a_2 = \frac{-\alpha_1\nu_1 J_0(\nu_1 p)}{\alpha_2\nu_2 J_0(\nu_2 p)} a_1$$

$$\Gamma_b = \left[J_1(\nu_1 p)J_0(\nu_2 p)\alpha_2 \nu_2 p - J_1(\nu_2 p)J_0(\nu_1 p)\alpha_1 \nu_1 p\right] kpK_0(kp)$$

$$+ \left[J_0(\nu_1 p)J_0(\nu_2 p)\nu_1 p \nu_2 p(\alpha_2 - \alpha_1)\right] K_1(kp)$$

$$b_1 = \left[kpK_0(kp)J_1(\nu_1 p) + \nu_1 pK_1(kp)J_0(\nu_1 p)\right] a_1 + \left[kpK_0(kp)J_1(\nu_2 p) + \nu_2 pK_1(kp)J_0(\nu_2 p)\right] a_2$$

$$b_2 = \left[kpI_0(kp)J_1(\nu_1 p) - \nu_1 pI_1(kp)J_0(\nu_1 p)\right] a_1 + \left[kpI_0(kp)J_1(\nu_2 p) - \nu_2 pI_1(kp)J_0(\nu_2 p)\right] a_2$$

$$c_2 = \frac{I_1(ks)}{K_1(ks)} b_1 + b_2$$

The average power transferred to the plasma is given by

$$P = -\frac{1}{2} \int_{-a}^{a} E_\theta(s, z) \cdot j(z)(2\pi s)dz$$

Since $j(z)$ is zero for $L > |z| > a$, we can write

$$P = -\frac{1}{2} \int_{-L}^{L} E_\theta(s, z) \cdot j(z)(2\pi s)dz$$

And since $E_\theta(r, z)$ and $j(z)$ are expanded in the same orthogonal series, it is possible to write

$$P = -\pi s \sum_{n=0}^{\infty} \int_{-L}^{L} E_{\theta_n}(s, z) \cdot j_n(z)dz$$

In references 2 and 3 the wave fields were calculated for an infinitely long plasma column, and thermal effects were neglected. In this case the fields were represented as a Fourier integral

$$\underline{E}(r, z, t) = \frac{1}{\pi} \int_{-\infty}^{\infty} \underline{E}(r, k)e^{i(kz - \omega t)} dk$$

This integral was evaluated by a contour integral technique that gave solutions which were sums of the residues of the integrand. To evaluate the residues, the zeros of the functions Γ (see preceding page) had to be found; and then the derivatives of Γ with respect to k, $d\Gamma/dk$, evaluated. For cold plasmas, all the terms in $\Gamma(k)$ are real and it is relatively easy to find numerically the values of k (all of which are real) which satisfy $\Gamma(k) = 0$. These k values are the wave numbers for the natural modes of the plasma column. When damping mechanisms (thermal effects) are included in the analysis, all the terms in $\Gamma(k)$ may become complex; and in general the k values of the natural modes are complex numbers. It has been our experience that standard numerical techniques do not work well in finding the roots of $\Gamma(k) = 0$ when damping is great and the real and imaginary parts are comparable. This is not to say it is impossible to find roots, just that it can be very time consuming.

The advantage of the technique used in this report, then, is that the zeros of $\Gamma(k)$ do not have to be found. For long plasma columns, the Fourier series solutions effectively amount to a numerical integration of the above Fourier integral. In addition, the effects of boundaries near the ends of the Stix coil can be included to the extent that one believes in the boundary conditions imposed. For power coupling calculations in which end boundary conditions are not important (such as when magnetic beaches exist), the technique is most applicable.

APPENDIX B

APPROXIMATIONS OF PLASMA DISPERSION FUNCTION

The calculations made in this report require the evaluation of the complex plasma dispersion function $Z(\xi)$ with ξ being pure real. For smaller values of the argument ($\xi < 3$) and for the calculations presented in table I and figures 5 to 7, the continued fraction approximation of Derfler and Simonen (ref. 5) was used

$$Z'(\xi) = -2i\sqrt{\pi}\,\xi \exp(-\xi^2) - \frac{2\ \xi^2}{1+\frac{1}{2}-} \cdot \cdot \cdot \cdot \frac{n\xi^2}{2n - \frac{1}{2}+} \frac{\left(n-\frac{1}{2}\right)\xi^2}{2n + \frac{1}{2}-} \cdot \cdot \cdot$$

$$Z(\xi) = \frac{-Z'(\xi) + 2}{2\xi}$$

The curves in figures 2 to 4 are from a previous report in which, for small arguments, the two-pole approximation (ref. 6) was used.

$$Z(\xi) = \frac{\left[\frac{1}{\alpha(\alpha - \xi)} - \frac{1}{\alpha^*(\alpha^* + \xi)}\right]}{1.10}$$

$$\frac{1}{\alpha} = 0.55 + i\sqrt{\frac{\pi}{2}}$$

The change to the continued fraction was made because it was discovered to be more accurate in the range of interest. For larger arguments ($\xi > 3$), and for all the calculations, the asymptotic expansion was used (ref. 1, ch. 8).

$$Z(\xi) = i\sqrt{\pi} \exp(-\xi^2) - \frac{1}{\xi}\left[1 + \frac{1}{2\xi^2} + \frac{3}{4\xi^2} + \cdot \cdot \cdot \cdot\right]$$

REFERENCES

1. Stix, Thomas H.: The Theory of Plasma Waves. McGraw-Hill Book Co., Inc., 1962.

2. Sigman, Donald R.; and Reinmann, John J.: Ion Cyclotron Wave Generation in Uniform and Nonuniform Plasma Including Electron Inertia Effects. NASA TN D-4058 1967.

3. Hosea, J. C.; and Sinclair, R. M.: Ion Cyclotron Wave Generation in the Model C Stellarator. Rep. MATT-673, Princeton Univ., June 1969.

4. Sigman, Donald R.: Calculations of Ion Cyclotron Wave Properties in Hot Plasmas. Bull. Am. Phys. Soc., vol. 14, no. 11, Nov. 1969, p. 1020.

5. Derfler, Heinrich; and Simonen, Thomas C.: Higher-Order Landau Modes. Phys. Fluids, vol. 12, no. 2, Feb. 1969, pp. 269-278.

6. Hedrich, C. L.; Fried, Burton D.; and McCune, James E.: Two-Pole Approximation for the Plasma Dispersion Function. Bull. Am. Phys. Soc., vol. 13, no. 2, Feb. 1968, p. 310.

NASA-Langley, 1971 —— 25 E-6080

"The aeronautical and space activities of the United States shall be conducted so as to contribute . . . to the expansion of human knowledge of phenomena in the atmosphere and space. The Administration shall provide for the widest practicable and appropriate dissemination of information concerning its activities and the results thereof."

—NATIONAL AERONAUTICS AND SPACE ACT OF 1958

NASA SCIENTIFIC AND TECHNICAL PUBLICATIONS

TECHNICAL REPORTS: Scientific and technical information considered important, complete, and a lasting contribution to existing knowledge.

TECHNICAL NOTES: Information less broad in scope but nevertheless of importance as a contribution to existing knowledge.

TECHNICAL MEMORANDUMS: Information receiving limited distribution because of preliminary data, security classification, or other reasons.

CONTRACTOR REPORTS: Scientific and technical information generated under a NASA contract or grant and considered an important contribution to existing knowledge.

TECHNICAL TRANSLATIONS: Information published in a foreign language considered to merit NASA distribution in English.

SPECIAL PUBLICATIONS: Information derived from or of value to NASA activities. Publications include conference proceedings, monographs, data compilations, handbooks, sourcebooks, and special bibliographies.

TECHNOLOGY UTILIZATION PUBLICATIONS: Information on technology used by NASA that may be of particular interest in commercial and other non-aerospace applications. Publications include Tech Briefs, Technology Utilization Reports and Technology Surveys.

Details on the availability of these publications may be obtained from:

SCIENTIFIC AND TECHNICAL INFORMATION OFFICE

NATIONAL AERONAUTICS AND SPACE ADMINISTRATION

Washington, D.C. 20546